Journal of Hydrology 380 (2010) 260–276

Contents lists available at ScienceDirect

Journal of Hydrology

journal homepage: www.elsevier.com/locate/jhydrol

Characterizing hydroclimatic variability in tributaries of the Upper Colorado River Basin—WY1911-2001

Margaret A. Matter *, Luis A. Garcia, Darrell G. Fontane, Brian Bledsoe

Department of Civil and Environmental Engineering, Colorado State University, Fort Collins, CO 80523-1372, United States

ARTICLE INFO

Article history:
Received 30 June 2009
Received in revised form 28 October 2009
Accepted 30 October 2009

This manuscript was handled by G. Syme, Editor-in-Chief

Keywords:
Hydroclimatic variability
Water supply forecasting
Nonstationarity
Colorado River Basin
Climate change
Land use/land cover/water use change

SUMMARY

Mountain snowpack is the main source of water in the semi-arid Colorado River Basin (CRB), and while the demands for water are increasing, competing and often conflicting, the supply is limited and has become increasingly variable over the 20th Century. Greater variability is believed to contribute to lower accuracy in water supply forecasts, plus greater variability violates the assumption of stationarity, a fundamental assumption of many methods used in water resources engineering planning, design and management. Thus, it is essential to understand the underpinnings of hydroclimatic variability in order to accurately predict effects of climate changes and effectively meet future water supply challenges.

A new methodology was applied to characterized time series of temperature, precipitation, and streamflow (i.e., historic and reconstructed undepleted flows) according to the three climate regimes that occurred in CRB during the 20th Century. Results for two tributaries in the Upper CRB show that hydroclimatic variability is more deterministic than previously thought because it entails complementary temperature and precipitation patterns associated with wetter or drier conditions on climate regime and annual scales.

Complementary temperature and precipitation patterns characterize climate regime type (e.g., cool/wet and warm/dry), and the patterns entail increasing or decreasing temperatures and changes in magnitude and timing of precipitation according to the climate regime type. Accompanying each climate regime on annual scales are complementary temperature (T) and precipitation (P) patterns that are associated with upcoming precipitation and annual basin yield (i.e., total annual flow volume at a streamflow gauge). Annual complementary T and P patterns establish by fall, are detectable as early as September, persist to early spring, are related to the relative magnitude of upcoming precipitation and annual basin yield, are unique to climate regime type, and are specific to each river basin. Thus, while most of the water supply in the Upper CRB originates from winter snowpack, statistically significant indictors of relative magnitude of upcoming precipitation and runoff are evident in the fall, well before appreciable snow accumulation.

Results of this study suggest strategies that may integrated into existing forecast methods to potentially improve forecast accuracy and advance lead time by as much as six months (i.e., from April 1 to October 1 of the previous year). These techniques also have applications in downscaling climate models and in river restoration and management.

© 2009 Elsevier B.V. All rights reserved.

Introduction

Water supply forecast accuracy for the Colorado River Basin decreased over the 20th Century due to increasing hydrologic and climatic variability in the system (Pagano et al., 2004; Jain et al., 2005). Winter mountain snowpack is the primary source of water supply of the CRB, and the limited and highly variable water supply must be allocated among diverse, increasing and often conflicting demands. Greater hydrologic variability also violates the assumption of stationarity, thereby invalidating many standard tools used in water resources planning, design and management (McCabe et al., 2007; Garfin et al., 2008; Milly et al., 2008). Therefore, identifying natural and anthropogenic sources of hydroclimatic variability in the CRB is central to accurately anticipating and adapting to the impacts on water supplies due to climate change (Chen and Grasby, 2009) and other anthropogenic activities. Most endeavors to improve forecast accuracy have involved advances in computing and new datasets, and while forecast accuracy has increased in some regions, such as the Northwest, accuracy has

* Corresponding author. Tel.: +1 970 491 7620; fax: +1 970 491 7626.
E-mail addresses: margaret.matter@colostate.edu (M.A. Matter), luis.garcia@colostate.edu (L.A. Garcia), darrell.fontane@colostate.edu (D.G. Fontane), brian.bledsoe@colostate.edu (B. Bledsoe).

0022-1694/$ - see front matter © 2009 Elsevier B.V. All rights reserved.
doi:10.1016/j.jhydrol.2009.10.040

decreased in other regions over the 20th Century (Pagano et al., 2004). Fresh approaches and methods are required to gain new insights into and understanding of hydroclimatic variability which may used to improve water supply forecast accuracy and increase lead time, as well as to develop new methods not based on stationarity for use in planning, design and management of water resources.

Increases in hydroclimatic variability are attributed primarily to anthropogenic climate change (e.g., Pagano and Garen, 2005; Garfin et al., 2008; Milly et al., 2008), but variability also arises from other sources, such as climate regimes and other forms of internal climate variability, air pollution (e.g., sulfate aerosols), modifications to land use, land cover and water use, and annual variability (Milly et al., 2008), as well as solar cycles (Kerr, 2009). In addition, sources of variability interact with one another, confounding detection and interpretation of variations in temperature and precipitation, as well as accurate representation of hydroclimatic processes in models for the CRB. Natural external forcings, such as solar cycles, and anthropogenic external forcings, including climate change and modifications to land use, land cover and water use, influence climate cycles (Wang and Schimel, 2003), or climate regimes. Effects of increasing greenhouse gas emissions since the start of the Industrial Revolution are particularly evident later in the 20th Century (Stott et al., 2000; Balling and Goodrich, 2007; Rosenzweig et al., 2008). Throughout the 20th Century, the CRB went through extensive changes in land use, land cover and water use, and during the same period, three climate regimes also occurred in the CRB (Hereford et al., 2002; Hidalgo and Dracup, 2003; McCabe et al., 2004; Balling and Goodrich, 2007). Since the three climate regimes during the 20th Century are also influenced by external forcings, including anthropogenic climate change and modifications to land use, land cover and water use, then it is reasonable to use climate regimes as a basis upon which to characterize hydroclimatic variability. In this way, changes in the hydroclimatic variables may be compared between climate regimes, as well as over the century.

Climate regimes and annual variations in the CRB are shaped by the combined effects of internal climate variability (e.g., climate modes), natural external forcings (e.g., solar variations); and anthropogenic external forcings (e.g., anthropogenic climate change; modifications to land use, land cover and water use; and air pollution, including sulfate aerosols and soot). Climate modes that evolve over longer time periods shape climate regimes, and climate modes that influence hydroclimate in the CRB include the Pacific Decadal Oscillation (PDO), Atlantic Mulidecadal Oscillation (AMO) and Pacific North American (PNA) (e.g., Hereford et al., 2002; Wang and Schimel, 2003; Woodhouse, 2003; Hidalgo, 2004; McCabe et al., 2004; Quiring and Goodrich, 2008). El Niño-Southern Oscillation (ENSO), on the other hand, evolves over shorter time periods and affects hydroclimate in the CRB on annual scales between fall and spring (e.g., Gershunov and Cayan, 2003; Hidalgo and Dracup, 2003; Balling and Goodrich, 2007; Kim et al., 2007). Yet expression of ENSO is modulated by factors including PDO and AMO, which evolve over longer time periods (McCabe and Dettinger, 1999; Gutzler et al., 2002; Gershunov and Cayan, 2003) and are influential drivers of hydroclimate in the CRB with or without contemporaneous ENSO extremes (Gershunov and Cayan, 2003). Because PDO and AMO evolve over long time periods, for example 20–30 years (Mantaua et al., 1997) and 50–80 years (e.g., Kerr, 2000; Enfield et al., 2001; McCabe et al., 2004; Quiring and Goodrich, 2008), respectively, they are unlikely to change substantially between fall and early spring. In contrast, ENSO evolves over shorter time periods (i.e., 2–7 years) and is phase-locked with the seasons so that ENSO conditions begin to set up in the Pacific in July; are established by about October and persist into early spring (Neelin et al., 2000). Thus ENSO conditions are relatively stable between fall and early spring.

It is then reasonable to assume that combined effects of AMO, PDO and ENSO, some of the major climate modes influencing hydroclimate in the CRB, are essentially stable between fall and early spring, meaning that temperature and precipitation patterns influencing snowpack development and snowmelt establish by fall and are detectable by October or earlier. This assumption is consistent with Hidalgo and Dracup (2003) and Archer and Fowler (2008) who found that April–September streamflow for the upper CRB and the River Jhelum in Pakistan, respectively, is more correlated with total precipitation for October–January than with any other time period (e.g., October–March, December–March, January–March, or October–September). The upper CRB and the River Jhelum are both snowmelt-dominated river systems and are influenced by ENSO at least during the winter months (e.g., Gershunov and Cayan, 2003; Hidalgo and Dracup, 2003; Balling and Goodrich, 2007; Kim et al., 2007; Archer and Fowler, 2008. Thus, similar to climate regimes which are characterized by prevailing temperature and precipitation patterns (e.g., cool/wet and warm/dry climate regimes), combined effects of major climate modes influencing annual hydroclimate in the CRB also entail complementary temperature and precipitation patterns that establish by fall, persist to early spring, and are associated with total upcoming precipitation and annual basin yield (ABY).

Internal climate variability occurs on all time scales from instantaneous to thousands of years, involving atmospheric and oceanic processes, and the coupled interactions between the ocean and atmosphere include climate modes, such as ENSO, PDO and AMO (Hegerl et al., 2007). Combined effects of climate modes influencing hydroclimate and water resources in the CRB (e.g., PDO and AMO) shape cool/wet or warm/dry climate regimes lasting approximately 30 years, and which are evident in double mass plots of cumulative precipitation and cumulative streamflow for coincident time periods. In turn, ENSO conditions combine with AMO and PDO to influence hydroclimate in the CRB on annual scales (e.g., Gershunov and Cayan, 2003; Hidalgo and Dracup, 2003; Balling and Goodrich, 2007; Kim et al., 2007).

Variations in the 11-year solar cycle, a natural external forcing, affect ENSO conditions. The solar maxima gives rise to La Niña-like and lagged El Niño-like conditions in the Pacific region, which may amplify or dampen true La Niña and El Niño conditions (Meehl and Arblaster, 2009). Effects of anthropogenic external forcings may vary temporally and spatially, depending on characteristics of the forcing and site specific conditions. For example, urban and agricultural irrigation may depress maximum daily temperatures locally or regionally, and the effects may be seasonal or longer (e.g., Pielke and Avissar, 1990; Stohlgren et al., 2003; Chase et al., 1999; Bounoua et al., 2000, 2002; Marland et al., 2009; Feddema et al., 2005; IPCC, 2007). Hence, natural and anthropogenic external forcings influence and change details of characteristic complementary temperature and precipitation patterns accompanying climate regimes so that complementary patterns for climate regimes of the same type (e.g., cool/wet climate regime) are similar but not alike.

Detecting climate signals in temperature, precipitation and streamflow records depends on factors including: (a) length and starting point of data records, (b) elevation of data gauges, and (c) level of impairment of the river basin above the gauge. As a guideline for minimizing misleading results, the length of hydrometeorological time series should be at least as long as the most prominent climate mode influencing hydroclimate in the area of interest, and the starting point of analysis in the time series relative to the phase of cyclic hydroclimatic component affects interpretation of results (Chen and Grasby, 2009). The most prominent climate mode is the AMO, and the collective effects of the phase of AMO and other climate modes give rise to climate regimes. The three climate regimes of the 20th Century in the CRB are: (1) a cool/wet climate

regime, from about 1905 to 1941; (2) a warm/dry climate regime, from about 1942 to 1977; and (3) a second cool/wet climate regime, from approximately 1978 to 1998 (e.g., Hereford et al., 2002; Hidalgo and Dracup, 2003; McCabe et al., 2004; Balling and Goodrich, 2007). Thus selecting time series for analysis that encompass most or all of the 20th Century would include the three main climate regimes of the Century and approximately two AMO cycles.

Previous studies have demonstrated that site elevation is an important factor in detecting climate signals. June–November ENSO conditions only correlate highly with October–March precipitation from high elevation sites in the upper CRB (Hidalgo and Dracup, 2003), and it has been observed that some models, such as snowmelt runoff models, may be improved significantly by including precipitation and temperature data from high elevation sites (Colle et al., 2000; Reed et al., 2001; Dracup, 2005). Other corroborating evidence includes tree ring data from higher elevation areas in China that exhibit less variability than trees at lower elevations (Wang et al., 2005). A large amount of variability is associated with the planetary boundary layer (PBL), the lower troposphere ranging between the earth's surface and approximately 300–10,000 ft in elevation. Within the PBL, air masses and transport processes are influenced by surface features (e.g., trees, mountains, buildings and water bodies) and by surface processes (e.g., evaporation, transpiration, diurnal temperature variations; Stull, 1988), as well as by effects of land surface modifications (Chase et al., 1999) and water use changes, which confound detection of climate signals. Above the PBL is the free atmosphere where air masses and transport processes are less affected by surface features, processes and modifications. Thus confounding effects of the PBL on climate signals are minimized by selecting gauges located at higher elevations.

Amount and spatial extent of modifications to land use, land cover and water use are greater at lower elevations than at higher elevation sites. The USGS Hydro-Climatic Data Network (HCDN) lists streamflow gauges with data records that are sufficiently unaffected by anthropogenic activities, and thus suitable for climate studies (Slack and Landwehr, 1992). Since land and water development tend to decrease with elevation, most of the HCDN gauges in the CRB are above 1829 m (6000 ft), and the related drainage basins are relatively small (i.e., between 518 and 3108 square kilometers (200 and 1200 square miles)). Basins at higher elevations tend to be more sensitive to change than basins at lower elevations for reasons including thinner soils, cooler temperatures, steeper terrain, higher UV radiation, and shorter growing seasons (Diffenbaugh, 2005; Brandt and Townsend, 2006). In addition, type of modification in a basin at higher elevations is at least as important as spatial extent of the modification (Dow, 2007), and the magnitude of effects of modifications correlates positively with elevation and correlates inversely with basin size (Monaghan et al., 2000; Brandt and Townsend, 2006). However, modifications to land use, land cover, and water use (e.g., irrigated agriculture) that occur at lower elevations also affect climate regionally, including adjacent mountain areas (e.g., Pielke and Avissar, 1990; Stohlgren et al., 2003; Chase et al., 1999; Bounoua et al., 2000, 2002; Marland et al., 2009; Feddema et al., 2005; IPCC, 2007). Nonetheless, higher elevation gauges may be better suited for detecting climate signals because confounding effects of the PBL may be less than at lower elevations.

The objectives of this research are to examine hydrometeorological time series for three climate regimes during the 20th Century for two gauges in the Upper CRB in order to: (a) identify patterns in the time series accompanying each climate regime; (b) identify changes in climate regime patterns over the century and potential causes of the changes, such as anthropogenic external forcings; (c) identify complementary patterns in temperature (T) and precipitation (P) between September and March that are associated with upcoming precipitation and ABY for each climate regime; and (d) develop multiple linear regression models, based on the complementary T and P patterns, to predict ABY for each of the three climate regimes of the 20th Century.

Site description

Tributaries and associated weather and streamflow gauges in the Upper CRB were selected according to the following considerations:

(a) Sites have concurrent temperature, precipitation and flow data.
(b) Data records encompass all or the majority of each climate regime of the 20th Century.
(c) Data are at daily time increments.
(d) Large-scale climate modes influencing climate at each site.
(e) Gauge elevation (i.e., over 1524 m (5000 ft)).
(f) Availability of reconstructed undepleted (naturalized) flow records for the flow gauges.

Weather and flow data for two sites in the Upper CRB, the Gunnison River near Gunnison, CO and Yampa River at Steamboat Springs, CO, are used for analysis and locations of the sites are indicated in Fig. 1.

The Gunnison River flows approximately east to west through the central Upper CRB and joins the Colorado River near Grand Junction, CO. The weather and stream gauges are located on the east side of the basin near the city of Gunnison, below the junction of the East and Taylor rivers, the two main tributaries forming the Gunnison River (see Fig. 1). North of the headwaters of the Gunnison River, is the Yampa River which flows west–southwest through Colorado and joins the Green River, a major tributary to the Colorado River, in Utah. Table 1 summarizes gauge and river basin information for the Gunnison and Yampa rivers. Both gauges are at elevations over 1829 m (6000 ft), and both drainage basins are relatively small, although the basin above the Yampa River gauge is about half the area of the basin above the Gunnison River gauge (see Table 1).

Since the streamflow records for the gauges, Gunnison River near Gunnison, CO (GRG) and Yampa River at Steamboat Springs, CO (YRS), are both part of the USGS HCDN, they are considered relatively unaltered by anthropogenic activities, and thus suitable for climate studies (Slack and Landwehr, 1992). However, the drainage basins above the GRG and YRS sites experienced land and water resource development over the 20th Century. Histories of the Gunnison and Yampa river basins include mining, timber harvesting, livestock grazing and agriculture during the first half of the 20th Century, and during the second half, the economies of both river basins depend largely on industries such as agriculture, grazing, coal mining, tourism, and recreation, including alpine skiing. In addition, because of local deposits of high-grade coal in the Yampa River Basin, the coal is mined and used to generate electrical power at large coal-fired power plants built upwind of the YRS site during the latter part of the century. Throughout the 20th Century, river diversions, including transbasin diversions, are used for agriculture, livestock, and other purposes, and later in the Century, diversions are also used for snowmaking at ski areas. Transbasin diversions from the Gunnison River Basin to the Colorado Front Range began in 1914. In 1936, Taylor Park dam and reservoir were completed upstream of the GRG gauge on the Taylor River, one of the main tributaries forming the Gunnison River. Taylor Park dam was built during the part of the GRG period of record that is discontinuous. Thus the WY 1911–1928 streamflow record does not

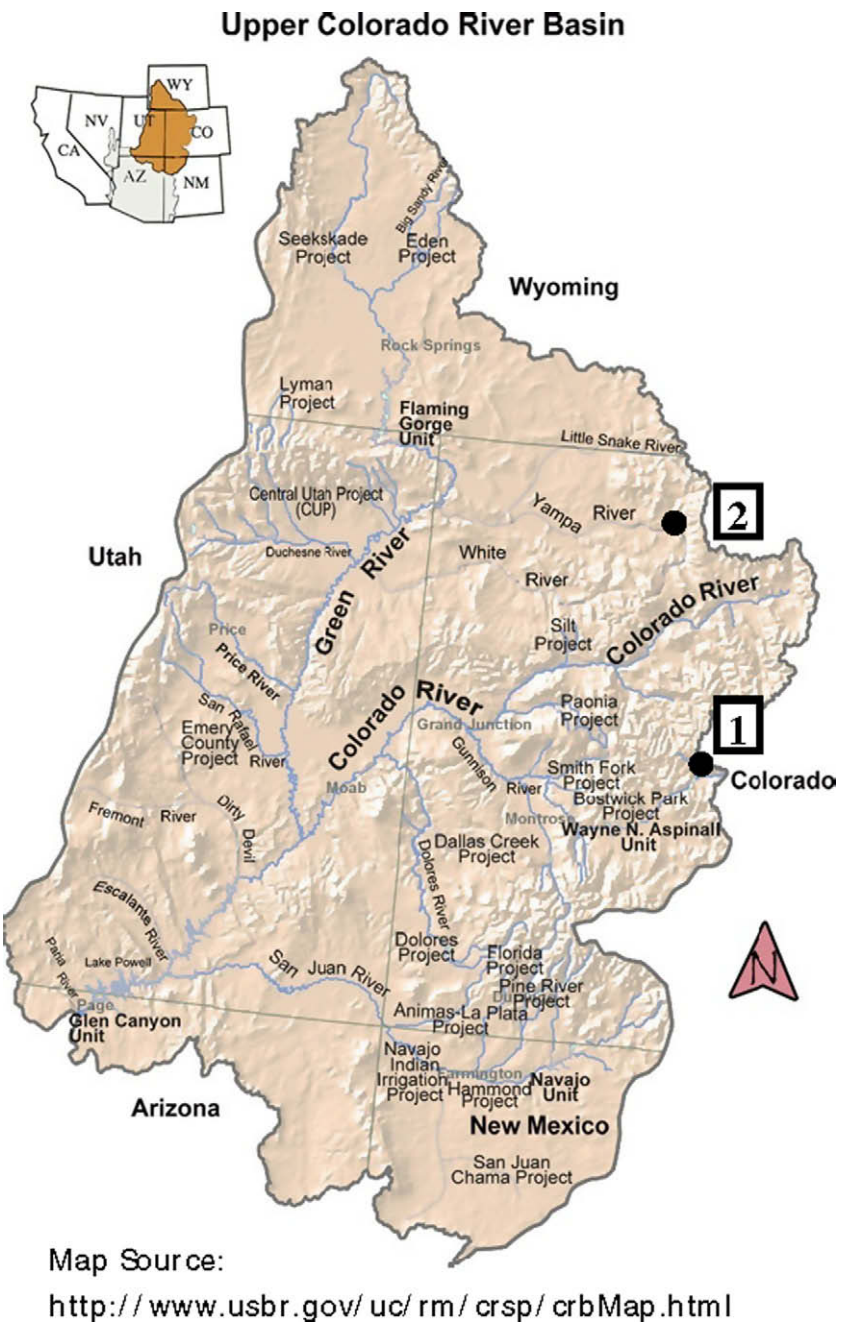

Fig. 1. The map of the Upper Colorado River Basin shows approximate locations of the two research gauges, the Gunnison River near Gunnison, CO [1] and Yampa River at Steamboat Springs, CO [2].

Table 1
River Basin and gauge information and periods of record.

USGS gauge name	USGS gauge no.	NWS gauge COOPID	Gauge elev. (ft)	Basin area (sq mi)	Period of record (in water years)		
					UB[a] cool/wet (*n* years)	AB[b] warm/dry (*n* years)	AB cool/wet (*n* years)
Gunnison River near Gunnison, CO	09114500	53,662	7655	1012	1911–1928 (18)	1945–1974 (30)	1975–2005 (31)
Yampa River at Steamboat Springs, CO	09239500	57,936	6695	568	1911–1942 (32)	1943–1974 (32)	1975–2005 (31)

[a] UB = unaltered basin.
[b] AB = altered basin.

include upstream reservoir operations but does include potential effects of transbasin diversions. Taylor Park Reservoir has no carry-over storage, so inflow is released primarily during the growing season for crops. In the Yampa River Basin, about six dams were

built upstream of the YRS gauge during the 20th Century. Most of the dams are relatively small, and water uses include agricultural irrigation, recreation, and municipal water supply.

Data and methods

Streamflow data were obtained online from the USGS National Water Information System at http://waterdata.usgs.gov/usa/nwis/sw, and meteorological data were obtained online from the National Climate Data Center at http://www.ncdc.noaa.gov/oa/climate/stationlocator.html. Streamflow records for the Gunnison River near Gunnison and the Yampa River at Steamboat Springs are HCDN gauges. The periods of record for meteorological and streamflow data for the sites in the upper Gunnison and Yampa river basins begin in the early 1900s and continue through the present. The period of record for the YRS gauge is continuous, but the streamflow period of record for the GRG gauge is discontinuous between October 1928 and September 1944. Despite the discontinuity, the period of record for the Gunnison River site is used because the early part of the flow record includes much of the cool/wet climate regime at the beginning of the 20th Century and the warm/dry climate regime during the mid-century, and the remainder of the record is good quality. Plus the Gunnison River is uniquely situated relative to boundaries of climate modes that influence hydroclimate in the Upper CRB. Woodhouse (2003) describes hydroclimatic conditions in the Gunnison River basin as among the most variable in the CRB, due in part to the basin location, which is near the border of the bipolar effects of ENSO and near the boundary of the PNA. In that regard, the Gunnison River basin may represent a "worst case scenario" for detecting climate signals. In contrast to the Gunnison River basin, the Yampa River basin is influenced more by La Niña conditions (Woodhouse, 2003).

Three climate regimes occur during the 20th Century in the CRB, and the research period of record, water year WY 1911–2005, is divided into three sub-periods of record, each coinciding approximately with a climate regime. The sub-period of record defining each climate regime also corresponds to different levels of development of land and water resources, or alteration in the basins. Accordingly, each of the three sub-periods of record is named for the prevailing climate regime and relative level of basin alteration. The unaltered basin (UB)-cool/wet climate regime is the sub-period of record that encompasses the cool/wet climate regime during the first third of the century, and involves a period of relatively limited development in the Gunnison and Yampa river basins (i.e., relatively unaltered basin conditions). Next, during the middle of the century is the altered basin (AB)-warm/dry climate regime, the sub-period of record which mainly entails the warm/dry climate regime, and is also a period of water and land resource development, or basin alteration. During the last third of century is the altered basin (AB)-cool/wet climate regime, the sub-period of record which encompasses the second cool/wet climate regime and includes further alteration of basin water and land resources. Table 1 summarizes information about the climate regime periods of record for the GRG and YRS sites.

During several years near the end of the WY 1911–2005 period of record, the climate regime changes from the AB-cool/wet to another warm/dry regime. The reasons for incorporating the period of transition between climate regimes are: (a) the assumption that the transition period between climate regimes, which began in about 1998, would not substantially impact analysis results; (b) the sub-periods of record would all be about the same length, and (c) to include more recent years of record.

In addition to historic gauge streamflow data, we assess whether climate signals are also evident in reconstructed undepleted flows, also referred to as "natural" or naturalized flows. Reconstructed undepleted streamflow data are historic gauge flow records adjusted for anthropogenic activities, such as irrigation diversions, transbasin imports, exports of water, reservoir operations, and estimated return flows. Reconstructed undepleted flows are used in water supply forecasting and other water resource management activities. Several entities develop reconstructed undepleted flow datasets, but the same gauges are not used by each of the entities and most of the data are developed at average monthly time increments. Daily data are required for this research and available from the Colorado Water Conservation Board (CWCB) for the GRG and the YRS sites. Although the CWCB does not develop water supply forecasts, they use reconstructed undepleted flow data for other water supply-related purposes. The undepleted flow records for GRG and YRS sites correspond to gauge data for 1975–2005, which is the calibration period of record for CWCB models. CWCB reconstructed undepleted flow datasets were developed by adjusting historic mean monthly streamflow data for diversions, return flows, transbasin imports and exports of water, and reservoir storage. Monthly undepleted flows are disaggregated to daily values using the pattern gauges, Yampa River at Steamboat Springs, CO for the YRS site, and the East River at Almont, CO for the GRG site (Colorado Water Conservation Board, 2004a,b). Undepleted flow data for WY 1975–2005 for the YRS and for the GRG sites are used in analysis, and this period of record coincides with the AB-cool/wet climate regime.

Temperature, precipitation and flow variables include mean and median monthly values (e.g., mean and median September maximum daily temperature), seasonal variables (e.g., January–March total cooling degree-days or September–December total precipitation), and annual variables for flow and precipitation. Heating and cooling degree-days are based on 0 °C (32 °F). One-third and one-half dates for quantities, including total annual and seasonal flow volumes, total precipitation, total seasonal heating degree-days and cooling degree-days, are the dates by which one-third or one-half of the quantities occur. For example, the January–March one-third precipitation date is the date by which one third of the total January–March precipitation arrives. Table 2 summarizes temperature, precipitation and flow variables used in analysis.

Unique attributes of the methodology include: (a) analyses are conducted from September through March, rather than the main snowpack accumulation months (i.e., December–March, or DJFM), or the main snowmelt runoff period (April–September); (b) rather than using one long period of record (e.g., WY 1911–2005) for analysis, the research period of record is divided into three sub-periods

Table 2
Summary of acronyms and abbreviations.

Term	Acronym or abbreviation
Altered basin	AB
Annual basin yield	ABY
Atlantic multidecadal oscillation	AMO
Colorado River Basin	CRB
Colorado Water Conservation Board	CWCB
Complementary temperature and precipitation patterns	Complementary T and P patterns
December, January, February and March	DJFM
El Niño/Southern oscillation	ENSO
Gunnison River near Gunnison, CO	GRG
Hydro-Climatic Data	HCDN
Maximum daily temperature	T_{max}
Minimum daily temperature	T_{min}
Mean/median daily	T_{daily}
Pacific Decadal Oscillation	PDO
Pacific North American	PNA
unaltered basin	UB
Water year	WY
Yampa River at steamboat springs, CO	YRS

of record, each corresponding approximately with one of the main climate regimes of the 20th Century; (c) results for each climate regime may be compared to identify similarities and differences between climate regimes, and to identify potential effects of anthropogenic external forcings on the climate regimes; (d) the sites are at higher elevations, minimizing confounding effects of the PBL, including effects of development at lower elevations in the basin; (e) methods are applied to reconstructed undepleted and actual gauge streamflow records; and (f) analyses are conducted at individual sites in a basin to determine whether the climate signal at a point is representative of the associated basin.

Nonparametric methods are included because the sub-periods of record are relatively short and some of the data are skewed. The methods are applied to temperature, precipitation and to historic and undepleted flow data between September and March for each year of each of the three climate regimes. Two seasons are defined for the September–March time period; Fall–Early Winter is September–December and October–December, and Winter–Early Spring is January–March. The Fall–Early Winter season is defined by two time periods because the current research suggested that climate signals are detectable earlier than October. Quartile analysis includes the mean, as well as the median, and is applied to temperature, precipitation and streamflow time series for each climate regime to examine differences in patterns of hydroclimatic variables between climate regimes of different types (e.g., cool/wet vs. warm/dry) and between climate regimes of the same type (e.g., UB-cool/wet vs. AB-cool/wet) to identify differences in climate regime patterns between climate regime types, and differences in patterns that may be associated with anthropogenic external forcings (e.g., climate change or modifications to land and water use).

Means and medians for each variable are compared using the Kruskal–Wallis Test ($\alpha = 0.05$; Helsel and Hirsch, 2002) to test whether the means and medians are the same for the climate regime periods of record and for the reconstructed undepleted flows. Spearman's ρ Rank Correlation ($\alpha = 0.02$; Helsel and Hirsch, 2002) is used to examine temperature associations with precipitation, flow and other temperature variables for September–March for each year of each climate regime. Significant associations between variables during a climate regime were used to develop complementary patterns in temperature and precipitation between September–March that are associated with relative magnitude of annual basin yield (ABY; total flow volume over a year at a stream gauge). The complementary *T* and *P* patterns are unique to each climate regime and are specific to each river basin.

Key components of the September–March complementary temperature and precipitation patterns were used to develop demonstration regression models for September–December and September–March to predict ABY for each of the three climate regimes. The AB-cool/wet climate regime period of record originally included several years of the warm/dry climate regime which began near the turn of the 21st Century (Schoennagel et al., 2007). Because the transition from the AB-cool/wet climate regime to the warm/dry climate regime of the 21st Century was estimated to occur over about 3 years, the AB-cool/wet climate regime record was truncated to WY 1975–2001 for the demonstration regression models.

Summary of results

Differences in median values between climate regimes

Generally, temperature and precipitation patterns change cyclically in concert with climate regimes. During the two cool/wet climate regimes (i.e., UB- and AB-cool/wet climate regimes) at both sites, temperatures are cooler overall, and total Fall–Early Winter precipitation is lower and is shifted earlier in the season, from November/December to September/October. Changes in total Winter–Early Spring precipitation between climate regimes varies between sites. At the GRG site, the total Winter–Early Spring precipitation is lower during the two cool/wet climate regimes, but at the YRS site, the Winter–Early Spring precipitation is higher. Fall–Early Winter and Winter–Early Spring seasonal flow volumes

Table 3
Comparison of median values for temperature between climate regimes at the GRG and YRS sites.

	GRG site				YRS site		
	UB-C/W[a] to AB-W/D[b]	AB-W/D to AB-C/W[c]	UB-C/W to AB-C/W		UB-C/W[a] to AB-W/D[b]	AB-W/D to AB-C/W[c]	UB-C/W to AB-C/W
Heating degree-days[d]				*Heating degree-days*			
September–December	ndc[e]	ndc	S +[f]	September–December	n +	S +	S +
October–December	S +	n –[g]	n +[g]	October–December	n +	ndc	n +
January–March	ndc	S +	S +	January–March	n +	S +	S +
Cooling degree-days[h]				*Cooling degree-days*			
October–December	S –[g]	n +	S –	October–December	S –	n +	n –
January–March	S –	ndc	S –	January–March	S –	S –	S –
Median daily temp.[i]				*Median daily temp.*			
September	n –	S +	n +	September	n –	S +	S +
October	S +	S –	S +	October	S +	ndc	S +
November	ndc	ndc	ndc	November	ndc	ndc	n +
December	S +	ndc	S +	December	ndc	ndc	ndc
January	S +	ndc	S +	January	ndc	n +	S +
February	S +	ndc	S +	February	ndc	S +	S +
March	S +	S +	S +	March	ndc	S +	S +

[a] UB-C/W = unaltered basin-cool/wet climate regime.
[b] AB-W/D = altered basin-warm/dry climate regime.
[c] AB-C/W = altered basin-cool/wet climate regime.
[d] Heating degree-days = based on 32 °F (0 °C).
[e] ndc = no discernible change.
[f] S +, S – = significant increase, significant decrease.
[g] n +, n – = not significant positive trend or negative trend.
[h] Cooling degree-days = based on 32 °F (0 °C).
[i] Temp. = temperature.

at the GRG site also change according to climate regime type; increasing in the cool/wet climate regimes and decreasing during the warm/dry climate regimes. However, at the YRS site seasonal flow volumes exhibit no significant changes between climate regimes (Tables 3–5). Opposite patterns in temperature and precipitation tend to prevail during the AB-warm/dry climate regime.

Long-term changes in temperature and precipitation over the 20th Century include:

(a) Temperatures increase in every month except November over the 20th Century at both sites (Table 3).
(b) Increases in temperature are most notable in minimum daily temperatures (T_{min}).
(c) Total heating degree-days (HDD) increase and total cooling degree-days (CDD) decrease in the Fall–Early Winter and Winter–Early Spring seasons at both sites (see Figs. 2–5).

Table 4
Comparison of median values for precipitation between climate regimes at the GRG and YRS sites.

	GRG site – comparison of precipitation variables between climate regimes				YRS site – comparison of precipitation variables between climate regimes		
	UB-C/W[a] to AB-W/D[b]	AB-W/D to AB-C/W[c]	UB-C/W to AB-C/W		UB-C/W[a] to AB-W/D[b]	AB-W/D to AB-C/W[c]	UB-C/W to AB-C/W
Annual precipitation				*Annual precipitation*			
	ndc[d]	S –[e]	n –[f]		S –	ndc	S –
Seasonal precipitation				*Seasonal precipitation*			
September–December	ndc	ndc	ndc	September–December	S +	S –	ndc
October–December	n +[f]	n –	n –	October–December	S +	n –	n +
January–March	S +[f]	S –	ndc	January–March	–	ndc	n –
Seasonal precipitation dates				*Seasonal precipitation dates*			
S-D[7] ½-precip.[8] date	S +	S –	ndc	S-D 1/2-precip. date	S +	S +	S +
O-D[7] 1/3-precip. date	ndc	n –	ndc	O-D 1/3-precip. date	S +	ndc	S +
Total monthly precipitation				*Total monthly precipitation*			
September	ndc	n +	n +	September	S –	S +	nd
October	n –	ndc	S –	October	S –	ndc	n –
November	S +	n –	ndc	November	S +	+	S +
December	ndc	S –	S –	December	n +	S –	n –
January	n +	ndc	n +	January	ndc	ndc	ndc
February	S +	n –	n +	February	n –	n –	S –
March	ndc	S –	S –	March	ndc	ndc	ndc

[a] UB-C/W = unaltered basin-cool/wet climate regime.
[b] AB-W/D = altered basin-warm/dry climate regime.
[c] AB-C/W = altered basin-cool/wet climate regime.
[d] ndc = No discernible change.
[e] S +, S – = significant increase, significant decrease.
[f] n +, n – = not significant positive trend or negative trend.

Table 5
Comparisons of median values of gauge flows between climate regimes and of median values of reconstructed flows with gauge flows for each climate cycle at the GRG and YRS sites.

	GRG site – comparison of gauge flows between climate regimes			GRG site – comparison of gauge and reconstructed undepleted flows		
	UB-C/W[a] to AB-W/D[b]	AB-W/D to AB-C/W[c]	UB-C/W to AB-C/W	RU[h]-AB-C/W UB-C/W	RU-AB-C/W AB-W/D	RU-AB-C/W AB-C/W
ABY	S –[d]	ndc[e]	S –	S –	S +	S +
WY 1/3-Q[f] Date	ndc	S –	n –[g]	S –	S +	S +
September–December Q vol.	S +[d]	S –	ndc	S –	S –	S –
October–December Q vol.	S –	S +	ndc	S –	S –	S –
January–March Q vol.	S –	S +	ndc	S –	S +	S –
	YRS site – comparison of gauge flows between climate regimes			GRG site – comparison of gauge and reconstructed undepleted flows		
	UB-C/W[a] to AB-W/D[b]	AB-W/D to AB-C/W[c]	UB-C/W to AB-C/W	RU-IC/W to UC/W	RU-IC/W to IW/D	RU-IC/W to IC/W
ABY	n –	ndc	n –	ndc	S +	S +
WY 1/3 Q date	ndc	n +[f]	ndc	ndc	S +	S +
September–December Q vol.	n –	ndc	S –	S –	ndc	ndc
October–December Q vol.	ndc	n –	S –	S –	n –	ndc
January–March Q vol.	S –	n –	S –	S –	n +	n +

[a] UB-C/W = unaltered basin-cool/wet climate regime.
[b] AB-W/D = altered basin-warm/dry climate regime.
[c] AB-C/W = altered basin-cool/wet climate regime.
[d] S +, S – = significant increase, significant decrease.
[e] ndc = no discernible change.
[f] Q = flow.
[g] n +, n – = not significant positive trend or negative trend.
[h] RU = reconstructed undepleted flows.

(d) Median annual precipitation decreases at both sites, but the initial decreases at each site occur at different times during the century (Table 4 and Fig. 6).
(e) Median ABY at both sites decreases during the 20th Century, and the decreases occur early in the 20th Century, between the UB-cool/wet and AB-warm/dry climate regimes (see Table 5 and Fig. 7).
(f) Median seasonal precipitation for September–December, October–December, and January–March exhibit some cyclic patterns at both sites corresponding to changes in climate regime, although Fall–Early Winter precipitation tends to change inversely with climate cycle type (see Table 4 and Figs. 8 and 9).

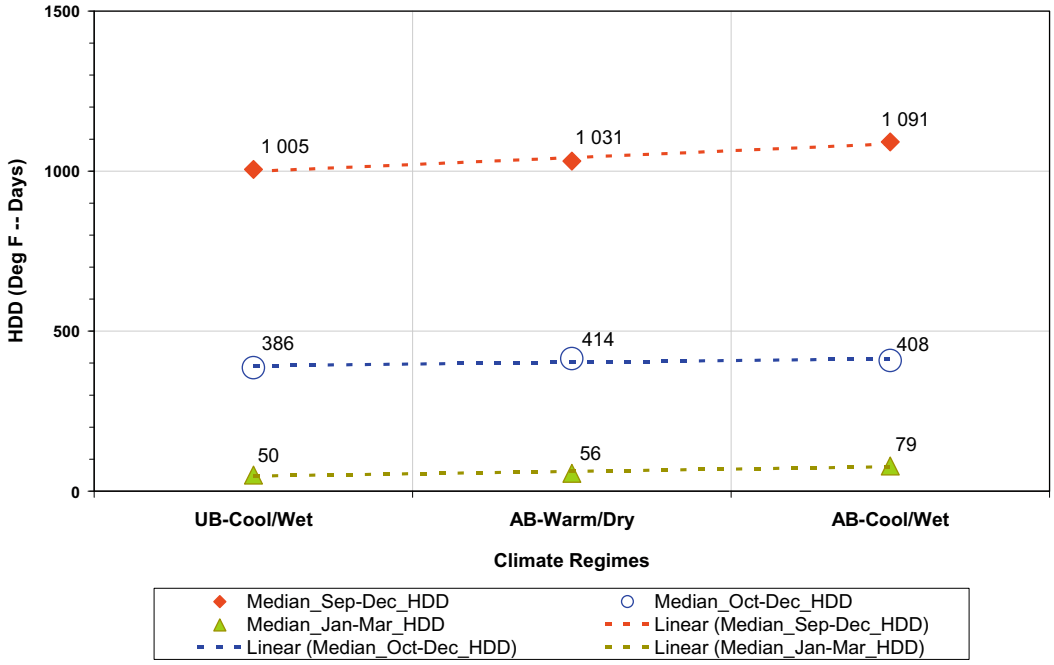

Fig. 2. Plots of median total heating degree-days (HDD) for September–December (solid diamonds), October–December (open circles), and January–March (solid triangles) for the three climate regimes at the YRS site show total HDD for September–December and January–March increase steadily and significantly over the 20th Century. October–December total HDD exhibit subtle cyclicity with climate regime type, but primarily exhibit an increasing trend over the century.

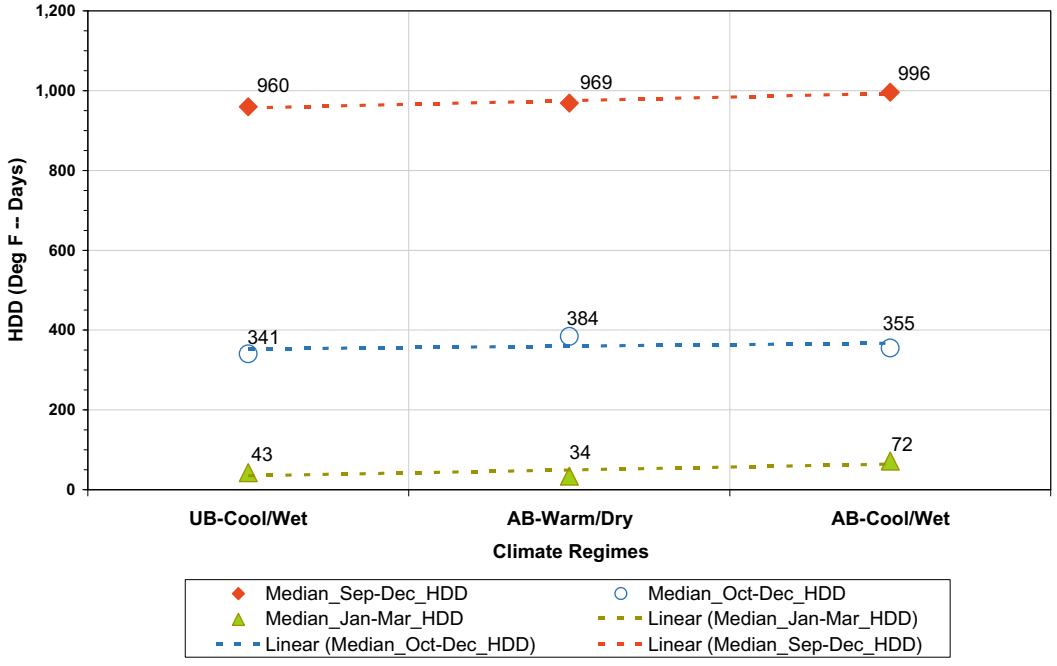

Fig. 3. Median total heating degree-days (HDD) for September–December (solid diamonds), October–December (open circles), and January–March (solid triangles) for the three climate regimes at the GRG site show that total HDD for September–December increase fairly steadily and significantly over the 20th Century, similar to the YRS site. October–December total HDD vary in accordance with climate regime type, January–March total HDD tend to vary inversely with climate regime type. Both October–December and January–March total HDD increase over the 20th Century; the increase is significant for January–March.

(g) October–December and January–March seasonal flow volumes change cyclically with the climate regimes at the GRG site, but decrease steadily over the 20th Century at the YRS site.

Climate signals associated with climate regimes are evident in results for the YRS and GRG sites, and even though both basins are relatively unaltered and located at higher elevations where confounding effects of the PBL are reduced, the results also exhibit evidence of anticipated effects of anthropogenic external forcings, including anthropogenic climate change and modifications to land cover and water use. Since higher elevation basins are typically more sensitive to change (Monaghan et al., 2000; Diffenbaugh, 2005; Brandt and Townsend, 2006; Dow, 2007), effects of local and regional changes in land use, land cover and water use, as well as anthropogenic climate change may be evident in changes over the 20th Century in temperature and precipitation patterns that accompany climate cycles.

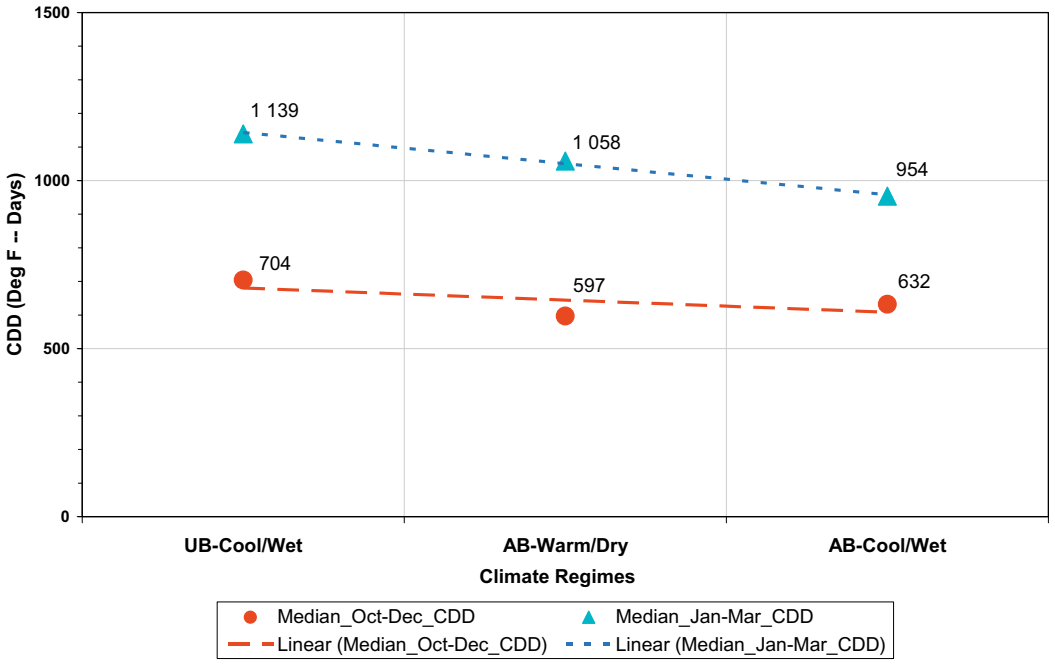

Fig. 4. October–December median total cooling degree-days (CDD; solid circles) for the YRS site exhibit cyclic variations in accordance with climate regime type, similar to total HDD, but also exhibit a negative trend over the 20th Century. January–March total CDD (solid triangles) decrease steadily and significantly over the century.

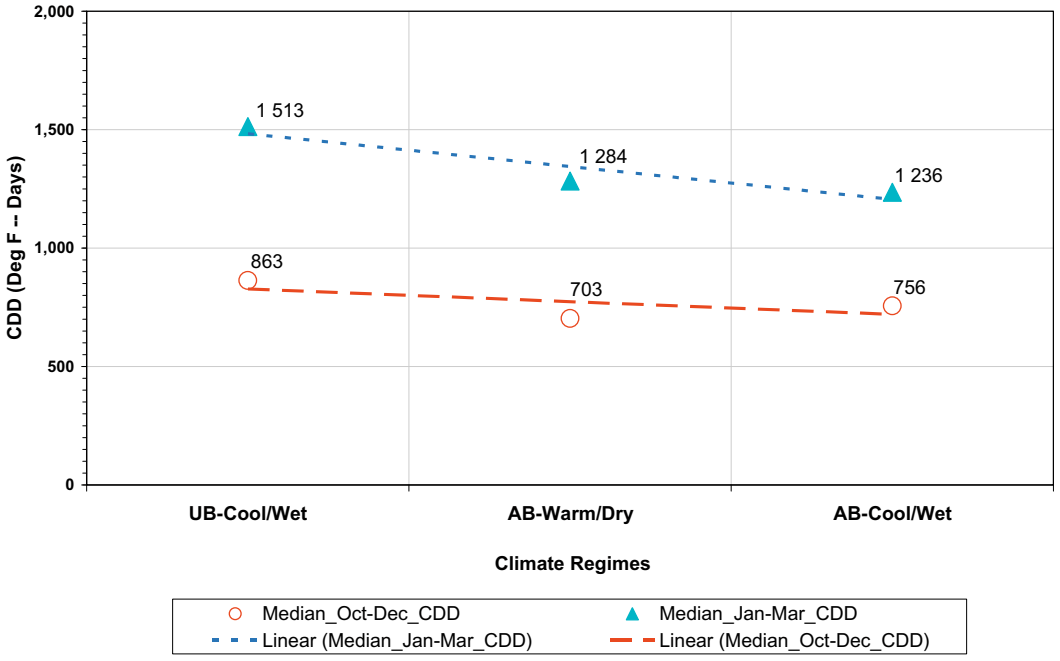

Fig. 5. Total cooling degree-days (CDD) for the October–December (open circles) and January–March median (solid triangles) for the GRG site exhibit cyclic variations in accordance with climate regime type, and decrease significantly over the 20th Century.

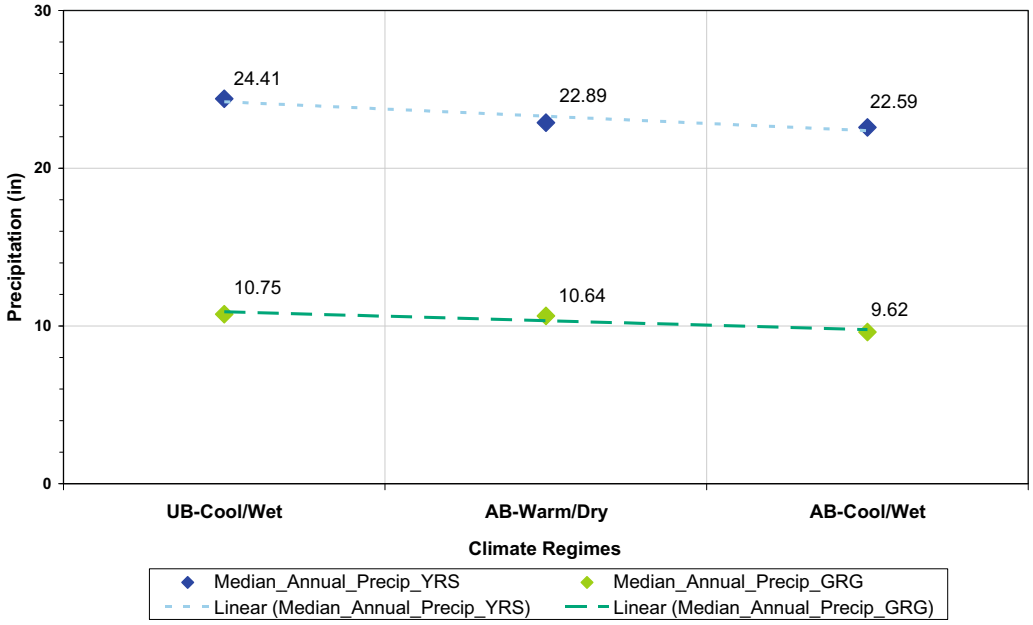

Fig. 6. The plot of median annual precipitation for the YRS site (black diamonds) and GRG site (grey diamonds) shows that median annual precipitation decreases significantly during the 20th Century at both sites, but the decreases at each site occur at different times. Median annual precipitation at the YRS site decreases significantly between the UB-cool/wet and AB-warm/dry climate regimes, but at the GRG site, annual precipitation decreases between the AB-warm/dry and AB-cool/wet climate regimes.

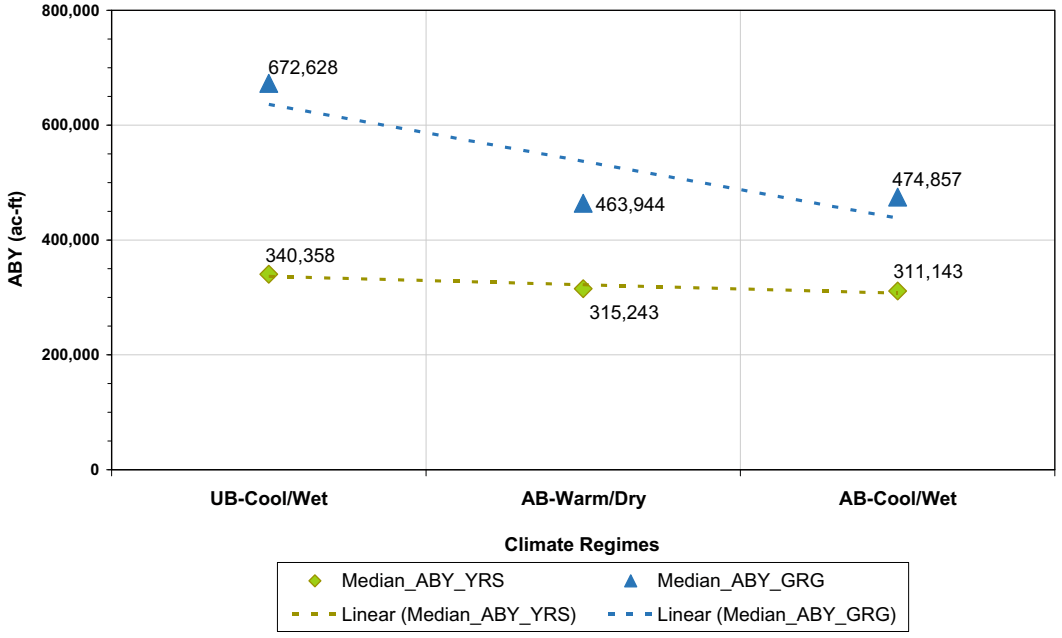

Fig. 7. Median annual basin yield (ABY) for the three climate regimes at the YRS site (solid diamonds) exhibits a negative trend, but at the GRG site (solid triangles), median ABY decreases significantly over the 20th Century.

Results for the undepleted flows are compared to those for actual gauge flows for the AB-cool/wet climate regime to determine differences between the undepleted and actual gauge flows for the same climate regime (i.e., AB-cool/wet), and results for undepleted flows are compared to those for the UB-cool/wet climate regime to identify differences between the undepleted flows and the relatively unaltered gauge flows for the UB-cool/wet climate regime.

Differences between reconstructed undepleted and actual gauge flows are evident on annual scales at both sites during the AB-cool/wet climate regime, but differences on seasonal scales vary between sites. Reconstructed undepleted ABY is significantly higher than actual gauge ABY during the AB-cool/wet climate regime at both sites. On seasonal scales, the undepleted flow volumes for the Fall–Early Winter and Winter–Early Spring seasons do not differ significantly from actual gauge flows at the YRS site, but are lower than gauge flows at the GRG site (Table 5).

Differences between reconstructed undepleted flows during the AB-cool/wet climate regime and actual gauge flows for the UB-cool/wet climate regime are considerable at the GRG site. Reconstructed undepleted ABY and seasonal flow volumes for the Fall–Early Winter and Winter–Early Spring seasons are significantly

lower and the undepleted WY 1/3-flow date is earlier than for actual gauge flows at the GRG site. At the YRS site, reconstructed undepleted ABY and actual gauge ABY do not differ significantly, but undepleted seasonal flow volumes for the Fall–Early Winter and Winter–Early Spring seasons are significantly lower than gauge seasonal flow volumes at the YRS site (Table 5).

Complementary T and P patterns

Spearman's ρ Rank Correlation was used to associate temperature with precipitation, streamflow and other temperature variables between September and March (September–March) for each climate regime. Significant associations were used to develop

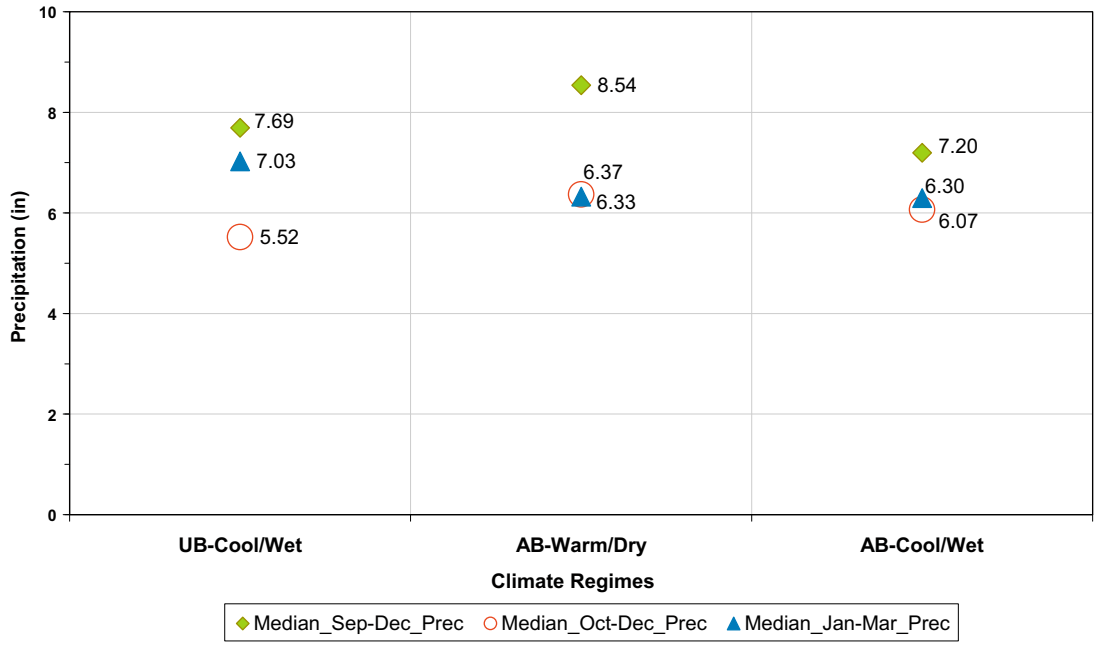

Fig. 8. Median total precipitation for September–December (solid diamonds) and for October–December (open circles) at the YRS site varies inversely with climate regime type; increasing during the warm/dry and decreasing during the cool/wet climate regimes. Over the 20th Century, October–December total precipitation exhibits a positive trend, but January–March total precipitation (solid triangles) primarily exhibits a negative trend.

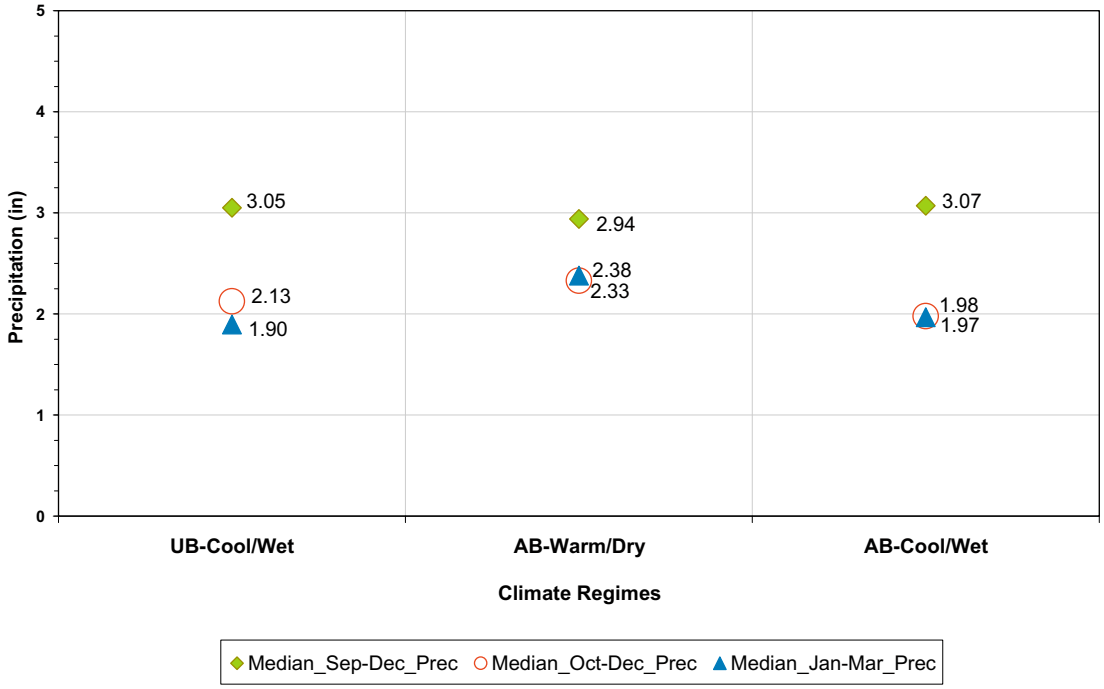

Fig. 9. Median total seasonal precipitation for September–December (solid diamonds) for the GRG site exhibits subtle, nonsignificant, variations with climate regime type. But October–December total precipitation (open circles) and January–March total precipitation (solid triangles) vary in contrast to climate regime type; increasing during the warm/dry and decreasing during the cool/wet climate regimes. Total precipitation for October–December also exhibits a negative trend over the 20th Century.

complementary patterns in temperature and precipitation (complementary *T* and *P* patterns) that are associated with relative magnitude of ABY during each climate regime. The September–March complementary *T* and *P* patterns associated with relative magnitude of upcoming precipitation and ABY are unique to climate regime type, specific to each river basin, and influenced by external forcings. Overall, characteristics of the complementary *T* and *P* patterns correspond with quartile results for temperature, precipitation and streamflow for each of the three climate regimes, and show that complementary *T* and *P* patterns for the UB- and AB-cool/wet climate regimes are similar, and they differ from patterns for the AB-warm/dry climate regime.

The September–March complementary *T* and *P* patterns are composed of three fundamental components: (a) early indicators, which are often minimum or maximum daily temperature or precipitation characteristics in September and October; (b) overall seasonal temperature conditions for the Fall–Early Winter and Winter–Early Spring seasons; and (c) timing of precipitation in the Fall–Early Winter and Winter–Early Spring seasons. For example, during the UB- and AB-cool/wet climate regimes at the GRG and YRS sites, higher ABY tends to accompany warmer minimum daily temperatures, which may yield mild temperature conditions overall in the Fall–Early Winter and Winter–Early Spring seasons, and precipitation begins earlier in the Fall-Early Winter season (i.e., September/October) (see Tables 3 and 4). In contrast, higher ABY during the AB-warm/dry climate regime at the GRG and YRS sites accompanies cooler maximum daily temperature in September and October, which may indicate cooler temperatures overall in the Fall–Early Winter and Winter–Early Spring seasons, and precipitation shifts later in the Fall–Early Winter season as a consequence of higher precipitation in December and lower precipitation in September/October (see Tables 3 and 4).

The temperature signal of the AB-cool/wet climate regime is also evident in the reconstructed undepleted flows on annual scales, but not seasonal scales, plus results for the reconstructed undepleted flows are occasionally in contrast to those for actual gauge flows. Since complementary *T* and *P* patterns are unique to each climate regime type, and the undepleted flows are developed for one climate regime (i.e., AB-cool/wet climate regime), temperature signals accompanying other climate regimes will not be detected in the reconstructed undepleted flow data.

Regression model predictions of ABY

Two regression models were developed using temperature and precipitation to predict ABY during each climate regime at the YRS and GRG sites, and the models and results are summarized in Tables 6 and 7. No transformations were made to the data, and temperature and precipitation are in English units. Results for the YRS and GRG sites show that the demonstration regression models are reasonably accurate in predicting ABY, and that most of the predictive information related to upcoming precipitation and ABY is typically detectable between September and December, rather than December to March. This corresponds with Hidalgo and Dracup (2003) and Archer and Fowler (2008) who found that April–September streamflow for the upper CRB and the River Jhelum in Pakistan, respectively, is more highly correlated with total precipitation for October–January than with any other time period (e.g., October–March, December–March, January–March, or October–September).

In general, the regression models for the UB- and AB-cool/wet climate regimes at the YRS site tend to explain more variance in ABY and are more accurate than the regression models for the AB-warm/dry climate regime. The September–December and September–March regression models explain about the same amount of variance in ABY; approximately 58–76% and 59–77%, respectively (Table 6). The most accurate models for the YRS site are the September–March demonstration model during the UB-cool/wet climate regime and the September–December demonstration model for the AB-cool/wet climate regime. Approximately 72% and 86% of the predictions of ABY by the September–March demonstration model for the UB-cool/wet climate regime are within 15% and 20%, respectively, of actual ABY. Similarly, approximately 74% and 78% of the predictions of ABY by the September–December demonstration model for the AB-cool/wet climate regime are within 15% and 20%, respectively, of actual ABY. Demonstration model results for reconstructed undepleted flows at the YRS site are similar to those for actual gauge flows during the AB-cool/wet climate regime (Table 6). Like the complementary *T* and *P* patterns, the demonstration model regression equations reflect changes in temperature, precipitation and streamflow between climate regimes. For example, the coefficient for September precipitation changes sign from negative to positive between the UB- and AB-cool/wet climate regimes, reflecting the change in amount and distribution of Fall–Early Winter precipitation over the 20th Century.

Similar to the YRS site, demonstration regression models for the GRG site are reasonably accurate for the three climate regimes (see Table 7). Yet in contrast to the YRS site, the two demonstration models for the AB-warm/dry climate regime at the GRG site tend to explain more variance in ABY, and the most accurate September–December demonstration model is also for the AB-warm/dry climate regime. Approximately 72% and 76% of the September–December model predictions of ABY are within 15% and 20%, respectively, of actual ABY.

Although the September–December and September–March demonstration models for the UB-cool/wet climate regime explain the least amount of variance in ABY, 43% and 58%, respectively, the most accurate September–March model is for the UB-cool/wet climate regime (see Table 7). Approximately 72% and 78% of the September–March regression model predictions of ABY are within 15% and 20%, respectively, of actual ABY. Despite reasonable accuracy of the demonstration models, the models tend to over-predict in drier conditions and under-predict in wetter conditions. This suggests that water losses in the upper Gunnison River Basin are higher in drier years and lower in wetter years than indicated by the relationships between hydroclimatic conditions and streamflow.

The September–December and September–March regression models were also applied to predict reconstructed undepleted ABY during the AB-cool/wet climate regime. The September–December and September–March demonstration models for the AB-cool/wet climate regime explain less variance and are usually less accurate at predicting reconstructed undepleted ABY than actual gauge ABY (see Table 7). The September–December and September–March demonstration models explain 58–61% of variance in reconstructed undepleted ABY, compared to 66–67% of the variance in actual gauge ABY. Predictions of reconstructed undepleted ABY are more accurate within 20% of actual reconstructed undepleted ABY than within 15% of actual reconstructed undepleted ABY. About 33% and 71% of September–December demonstration model predictions and 43% and 74% September–March model predictions of reconstructed undepleted ABY are within 15% and 20%, respectively, of actual reconstructed undepleted ABY.

Similar to demonstration regression model predictions of actual ABY, the September–December and September–March demonstration models tend to over-predict reconstructed undepleted ABY in drier years and under-predict in wetter years. Since the reconstructed undepleted flows are actual gauge flow adjusted for water management activities, the results suggest that the tendencies may be due to water losses and water management activities that were not included in or were under-estimated during development of the reconstructed undepleted flows. Unaccounted or under-ac-

Table 6
YRS site percent of predicted annual basin yield that is within 15% and 20% of actual ABY during the three climate regimes of the 20th Century.

Climate regime	September–March model[a] variables	r^2[b] September–March model	% Of predicted within 15% of actual ABY[b]	% Of predicted within 20% of actual ABY	September–December model[c] variables	r^2 September–December model	% Of predicted within 15% of actual ABY	% Of predicted within 20% of actual ABY
YRS site								
UB cool/wet	– September Prec.[d] – November Prec. – December T_{max}[e] – January Prec.	0.76	72	86	– September Prec. – October T_{max} – November Prec. – November T_{max}	0.69	66	79
AB warm/dry	– October T_{max} – November T_{max} – December Prec. – January Prec.	0.59	61	81	– October T_{max} – November T_{max} – November T_{min}[f] – December Prec.	0.58	58	74
AB cool/wet	– September Prec. – October Prec. – December Prec. – January Prec.	0.77	70	78	– September Prec. – October Prec. – October T_{min} – December Prec.	0.76	74	78
Undepleted Q AB cool/wet	– September Prec. – October Prec. – December Prec. – January Prec.	0.75	76	76	– September Prec. – October Prec. – October T_{min} – December Prec.	0.74	72	84
Demonstration regression model equations								
UB cool/wet	– September Prec.[d] – November Prec.-Dec T_{max}[e] – January Prec.	ABY = 512,027 + [(−18,884) ∗ September Prec.] + [(39,911) ∗ November Prec.] + [(−8587) ∗ December T_{max}] + [(28,566) ∗ January Prec.]			– September Prec. – October T_{max} – November Prec. – November T_{max}	ABY = 732,453 + [(−23,688) ∗ September Prec.] + [(−5953) ∗ October T_{max} + [(−1930) ∗ November T_{max}] + [(62,202) ∗ November Prec.]		
AB warm/dry	– October T_{max} – November T_{max} – December Prec. – January Prec.	ABY = 804,794 + [(−4629) ∗ October T_{max}] + [(−6428) ∗ November T_{max}] + [(17,283) ∗ December Prec.] + [(17,881) ∗ January Prec.]			– October T_{max} – November T_{max} – November T_{min} – December Prec.	ABY = 861,573 + [(−4948) ∗ October T_{max}] + [(−4911) ∗ November T_{max}] + [(−4926) ∗ November T_{min}] + [(22,141) ∗ December Prec.]		
AB cool/wet	– September Prec. – October Prec. – December Prec. – January Prec.	ABY = 100,164 + [(21,923) ∗ September Prec.] + [(51,451) ∗ October Prec.] + [(38,641) ∗ December Prec.] + [(10,607 ∗ January Prec.]			– September Prec. – October Prec. – October T_{min} – December Prec.	ABY = 188,326 + [(21,010) ∗ September Prec.] + [(57,015) ∗ October Prec.] + [(−2896) ∗ October T_{min}] + [(39,218) ∗ December Prec.]		
Undepleted Q AB cool/wet	– September Prec. – October Prec. – December Prec. – January Prec.	ABY = 149,078 + [(13,134) ∗ September Prec.] + [(48,748) ∗ October Prec.] + [(40,706) ∗ December Prec.] + [(13,873 ∗ January Prec.]			– September Prec.Prec. – October Prec. – October T_{min} – December Prec.	288,843 + [(13,212) ∗ September Prec.] + [(57,473) ∗ October Prec.] + [(−5021) ∗ October T_{min}] + [(41,570) ∗ December Prec.]		

[a] September–March model = regression model comprised of variables for September–March to predict ABY.
[b] ABY = annual basin yield.
[c] September–December model = regression model comprised of variables for September–March to predict ABY.
[d] Prec. = precipitation.
[e] T_{max} = maximum daily temperature.
[f] T_{min} = minimum daily temperature.

Table 7
GRG site percent of predicted annual basin yield that is within 15% and 20% of actual ABY during the three climate regimes during the 20th Century.

Climate regime	September–March model variables	r[b] September–March model	% Of predicted within 15% of actual ABY[a]	% Of predicted within 20% of actual ABY	September–December model variables	r[b] September–December model	% Of predicted within 15% of actual ABY	% Of predicted within 20% of actual ABY
UB cool/wet	– September median T_{daily}[c] – October Prec. January T_{min} – January Prec.	0.58	72	78	– September T_{daily} – October T_{min} – November Prec. – December T_{min}	0.43	0.67	0.72
AB warm/dry	– October median T_{daily} – November T_{max} – December T_{max} – January Prec.	0.67	62	72	– October median T_{daily} – November T_{max} – November T_{min} – December T_{max}	0.66	72	76
AB cool/wet	– October T_{min} – November Prec. – December T_{max} – February Prec.	0.66	64	77	– October T_{min} – November Prec. – December T_{max} – December T_{min}	0.67	48	61
Undepleted Q AB cool/wet	– October T_{min} – November Prec. – December T_{max} – February Prec.	0.58	43	74	– October T_{min} – November Prec. – December T_{max} – December T_{min}	0.61	33	71
Demonstration regression model equations								
UB cool/wet	– September median T_{daily}[c] – October Prec. – January T_{min} – January Prec.	ABY = −145,045 + [(16,521) ∗ September T_{daily}] + [(−49,038) ∗ October Prec.] + [(54,572) ∗ January Prec.] + [(7005) ∗ January T_{min}]			– September median T_{daily} – October T_{min} – November Prec. – December T_{min}	ABY = 88,767 + [(20,600) ∗ September T_{daily}] + [(−25,384) ∗ October T_{min}] + [(1597) ∗ November Prec.] + [(−2459) ∗ December T_{daily}]		
AB warm/dry	– October median T_{daily} – November T_{max} – December T_{max} – January Prec.	ABY = 2,117,210 + [(−22,413) ∗ October T_{daily}] + [(−12,288) ∗ November T_{max}] + [(−4478) ∗ December T_{max}] + [(41,557) ∗ January Prec.]			– October median T_{daily} – November T_{max} – November T_{min} – December T_{max}	ABY = 2,268,634 + [(−21,272) ∗ October T_{daily}] + [(−12,997) ∗ November T_{max}] + [(−9838) ∗ November T_{min}] + [(−5403) ∗ December T_{max}]		
AB cool/wet	– October T_{min} – November Prec. – December T_{max} – February Prec.	ABY = −136,226 + [(28,850) ∗ October T_{min}] + [(132,351) ∗ November Prec.] + [(−4561) ∗ December T_{max}] + [(245,889) ∗ February Prec.]			– October T_{min} – November Prec. – December T_{max} – December T_{min}	ABY = 1,146,194 + [(14,220) ∗ October T_{min}] + [(109,431) ∗ November Prec.] + [(−30,025) ∗ December T_{max}] + [(27,317) ∗ December T_{min}]		
Undepleted Q AB cool/wet	– October T_{min} – November Prec. – December T_{max} – February Prec.	ABY = −1959 + [(30,032) ∗ October T_{min}] + [(130,372) ∗ November Prec.] + [(−6595) ∗ December T_{max}] + [(161,692) ∗ February Prec.]			– October T_{min} – November Prec. – December T_{max} – December T_{min}	1,123,785 + [(17,703) ∗ October T_{min}] + [(102,962) ∗ November Prec.] + [(−29,792) ∗ December T_{max}] + [(26,091) ∗ December T_{min}]		

T_{min} = minimum daily temperature.
T_{max} = maximum daily temperature.
[a] ABY = annual basin yield.
[b] Prec. = precipitation.
[c] Median T_{daily} = median daily temperature.

counted water losses may include evapotranspiration, channel and conveyance losses, reservoir storage losses, and effects of transmountain and other diversions on ground water recharge. Moreover, these factors may vary with climate regimes and effects of external forcings, and the effects may be greater in the Upper Gunnison River Basin because of unique physiographic characteristics such as valley winds (Sato and Kondo, 1988; Hay, 1998) and permeable soils (Colorado State University, 2000). Given the elevation and unique physiographic characteristics of the Upper Gunnison River Basin, modifications to land use, land cover and water use in the basin may result in enhanced water losses, which may be greater than expected during drier conditions, but less than expected during wetter conditions.

Discussion and conclusions

We proposed an innovative methodology that characterizes hydroclimatic variability according to climate regimes, a fundamental part of internal climate variability and upon which external forcings act. Results show that hydroclimatic variability is more deterministic than previously thought because it entails complementary temperature (T) and precipitation (P) patterns on climate regime and annual scales that are related to wetter or drier conditions.

Stochastic processes, such as precipitation and streamflow, include both deterministic and random aspects (Salas et al., 1997), and the random aspect incorporates that which is unknown about deterministic processes. Conventional stochastic methods focus more on the random aspects, rather than the deterministic, and assume that natural variability occurs within a range so the mean essentially remains the same over time, or is stationary, and stochastic processes may be simulated probabilistically. Since the 1960s when development and use of stochastic methods escalated (Salas et al., 1997), knowledge and understanding of hydroclimatic processes has advanced, including that hydroclimatic processes are not stationary and variability increased over the 20th Century (McCabe et al., 2007; Garfin et al., 2008; Milly et al., 2008).

Results of this research demonstrate that, over the 20th Century, hydroclimatic variability during that time includes: (a) a sequence of alternating complementary temperature and precipitation patterns associated with changes between cool/wet and warm/dry climate regimes; and (b) differences in complementary patterns for climate regimes of the same type show evidence of anticipated or observed effects of some anthropogenic external forcings on the climate regimes. The results reveal relationships among hydrometeorological variables that are associated with individual climate regimes, which provide direction for determining the mechanisms behind the relationships. As understanding of the physics of hydroclimatic processes increases, the random aspect decreases, and the advances in understanding may be used to improve predictive methods to increase accuracy of and reduce uncertainty in predictions of climate and water supply.

The September–March complementary T and P patterns suggest circumstances associated with extreme conditions (i.e., wet or dry) for each climate regime, so key elements of the patterns were used to develop demonstration regression models to predict ABY for each year of each climate regime during the 20th Century at the YRS and GRG sites. September–December and September–March regression models for each climate regime accurately predict ABY at both sites, and most of the predictive information of ABY is detectable between September and December. Applications of the demonstration regression models to reconstructed undepleted flows for both sites indicate that adjusting gauge flows for water management activities and estimated return flows may not improve accuracy of predictions of ABY.

In addition, results of the demonstration regression models for actual gauge flows and reconstructed undepleted flows for the GRG site exhibit similar tendencies to over-predict in drier years and under-predict in wetter years. Since the demonstration models respond similarly for reconstructed undepleted and actual gauge flows, this suggests that water management activities and return flows are not the only factors affecting the relationship between hydroclimatic conditions and streamflows. Other influencing factors may include evapotranspiration, recharge, and channel and conveyance losses, reservoir storage losses, and effects of transmountain and other diversions on ground water recharge. Moreover, these factors may vary with cool/wet and warm/dry climate regimes, as well as effects of external forcings, and the effects may be greater in the Upper Gunnison River Basin because of unique physiographic characteristics such as valley winds (Sato and Kondo, 1988; Hay, 1998) and permeable soils (Colorado State University, 2000). Given the elevation and unique physiographic characteristics of the Upper Gunnison River Basin, modifications to land use, land cover and water use in the basin may result in enhanced water losses, which may be greater than expected during drier conditions, and less than expected during wetter conditions. This would explain demonstration model tendencies to over-predict in drier conditions and under-predict in wetter conditions.

Even though the Gunnison River Basin is one of the most hydroclimatically variable systems in the CRB (Woodhouse, 2003), the methodology used in this research accurately predicts ABY at the GRG site for the three climate regimes during the 20th Century. Thus, since the methods were successful for the Gunnison River Basin, then the same methods are likely to be successful in other basins of the CRB, and perhaps other river systems.

Identification of September–March complementary T and P patterns associated with total upcoming precipitation and ABY are consistent with findings of Hidalgo and Dracup (2003) and Archer and Fowler (2008) who determined that April–September streamflow in ENSO-influenced snowmelt-dominated river systems is more highly correlated with total precipitation for the preceding October–January than with any other time period (e.g., preceding October–March, December–March, January–March, or October–September). Correspondingly, incorporating SSTs and 500 mbar geopotential height indices in water supply forecasts have also been shown to increase lead time. For example, Grantz and others (2005) found that September–November SSTs and 500 mbar geopotential height in the northern mid-Pacific Ocean correlate with the upcoming April–July flow volume for the Carson River in Nevada, and Soukup and others (2009) showed significant correlations between the July–September AMO index and upcoming April–July streamflow for the North Platte River in Wyoming and Colorado.

Other studies have also used either flows for HCDN gauges or reconstructed undepleted (natural or naturalized) flows, but the time series were not divided according to climate regimes. Instead, flow data were assessed using moving average windows of various lengths that correspond with variations in different climate modes. Pagano and Garen (2005) assessed persistence and variability in April–September flow volumes for HCDN gauges over 20-year moving windows during the 20th Century, and Jain and others (2005) evaluated year-to-year variability in annual streamflow volumes over 30-year moving windows using naturalized flows. Although neither study associates the time windows with climate regimes or particular climate modes, results of both studies showed higher variability in flow volumes during the last 30 years of the 20th Century, which corresponds approximately to the AB-cool/wet climate regime in the Upper CRB used in this research. It is a time period during which effects of increases in greenhouse gases since the Industrial Revolution are particularly evident (Stott et al., 2000; Balling and Goodrich, 2007; Rosenzweig et al., 2008), and the cumulative effects of land and water resource development and other

anthropogenic external forcings are also evident. Results of our research show that adjusting gauge flows for water management activities and return flows may not improve predictions, and may not accurately detect trends or patterns. In addition, Chen and Grasby (2009) demonstrate that: (a) the length of time series relative to the periodicity of cycles, (b) magnitude and phase of the longest cycle, and (c) starting point of data records are important factors in accurately determining trends in hydroclimatic time series.

McCabe and others (2007) associated detrended 11-year moving averages of naturalized flows for gauges in the Upper CRB with sea-surface temperatures (SST) to determine relationships between decadal to multidecadal variability in SST and annualized flows for WY 1906–2003. The resultant streamflow time series depicts cyclic patterns about 30-years in length over the 20th Century that correspond approximately with the three climate regimes defined in our research. In addition, correlations between AMO SSTs and temperature and precipitation for the Upper CRB indicated that, when AMO is positive, precipitation is generally below average and temperatures are typically above average, which is consistent with results of quartile analysis for the AB-warm/dry climate regime at the YRS site, and temperature results for the GRG site. Median annual precipitation at the GRG site did not decrease during the AB-warm/dry climate regime, but the distribution of precipitation shifted during the seasons, which may have contributed to lower annual flows.

McCabe et al. (2007) also revealed 11-year periods of wet and dry conditions during the 1906–2003 period of record. Since the periodicity of AMO is the longest among the climate modes that influence hydroclimate in the CRB (i.e., 50–80 years (e.g., Kerr, 2000; Enfield et al., 2001; McCabe et al., 2004; Quiring and Goodrich, 2008)), the variations revealed by McCabe et al. (2007) may be related to magnitude, stage, or changes in phase of other climate modes that evolve over shorter periods of time, such as PDO and ENSO.

A large body of research establishes relationships between large-scale ocean–atmosphere interactions and water resources in CRB, but the relationships do not provide reliable predictions of water resources on seasonal scales, and the physical mechanisms driving the interactions are not sufficiently understood to improve prediction of future conditions (McCabe et al., 2007). The methodology described in this paper demonstrates that climate regimes, which are shaped by climate modes influencing hydroclimate in the Upper CRB, are a useful basis upon which to characterize hydroclimatic variability in the Upper CRB, and the methodology reveals complementary patterns in temperature and precipitation on climate regime and annuals scales that may be used to improve accuracy of predictions of upcoming water supplies and increase lead time as much as 6 months, from April 1 to October 1 of the previous year. In addition to water supply forecasting, the results of this research also have applications in: (a) downscaling climate models; (b) river restoration; (c) river system management; (d) improving methods used in water resources engineering that are based on the assumption of stationarity; and (e) by determining the factors driving recent increases in hydroclimatic variability, the results may also be used in developing long-rang decadal climate forecasts (Pagano and Garen, 2005).

Alternative strategies may be integrated into existing water supply forecast procedures to help improve forecast accuracy and advance lead time by as much as 6 months; from April 1 to October 1. Examples of applications include:

(a) Modify the 30-year flow reference period, which is used by the NRCS and NWS in the forecast procedures, from the last 30-years to coincide with the current climate regime, or a climate regime of the same type as the current climate regime that has been adjusted for relevant external forcings.
(b) Extend the period of analysis from December–March (DJFM) to September–March to incorporate the evolution of the complementary T and P pattern associated with upcoming precipitation and ABY.
(c) Include in the selection of regression variables those that are consistent with the complementary T and P patterns associated with ABY for the current climate regime and specific river basins.

Results of this research also indicate ways to improve reconstructed undepleted, or "natural" flow datasets, and may have applications in river restoration, water resource management, and in improving water resources engineering methods which are based on stationarity.

Acknowledgments

Our sincere gratitude to Dr. Jill Baron for her thorough reviews; insightful and substantive comments; direct and constructive guidance, and energetic support.

References

Archer, D.R., Fowler, H.J., 2008. Using meteorological data to forecast seasonal runoff on the River Jhelum, Pakistan. Journal of Hydrology 361, 10–23.
Balling Jr., R.C., Goodrich, G.B., 2007. Analysis of drought determinants for the Colorado River Basin. Climate Change 82, 179–194.
Bounoua, L., Collatz, G.J., Los, S.O., Sellers, P.J., Dazlich, D.A., Tucker, C.J., Randall, D.A., 2000. Sensitivity of climate to changes in NDVI. Journal of Climate 12, 2277–2292.
Bounoua, L., Defries, R., Collatz, G.J., Sellers, P., Khan, H., 2002. Effects of land cover conversion on surface climate. Climate Change 52, 29–64.
Brandt, J.S., Townsend, P.A., 2006. Land use–land cover conversion, regeneration and degradation in the high elevation Bolivian Andes. Landscape Ecology 21, 607–623.
Chase, T.N., Pielke Sr., R.A., Kittel, T.G.G., Baron, J.S., Stohlgren, T.J., 1999. Potential impacts on Colorado Rocky Mountain weather due to land use change on the adjacent Great Plains. Journal of Geophysical Research 104, 16673–16690.
Chen, Z., Grasby, S.E., 2009. Impact of decadal and century-scale oscillations on hydroclimatic trend analyses. Journal of Hydrology 365, 122–133.
Colle, B.A., Mass, C.F., Westrick, K.J., 2000. MM5 precipitation verification over the Pacific Northwest during the 1997–1999 cool seasons. Weather and Forecasting 15, 730–744.
Colorado State University (CSU) Cooperative Extension, 2000. Improving forage yields and quality in Colorado. Agronomy News 20, 1–14.
Colorado Water Conservation Board (CWCB), 2004a. Yampa River Basin Water Resources Planning Model User's Manual, June 2004, p. 8-7.
Colorado Water Conservation Board (CWCB), 2004b. Gunnison River Basin Water Resources Planning Model User's Manual, Appendix C, July 2004, p. C-4.
Diffenbaugh, N.S., 2005. Atmosphere-land cover feedbacks alter the response of surface temperature to CO_2 forcing in the western United States. Climate Dynamics 24, 237–251.
Dow, C.L., 2007. Assessing regional land-use/cover influences on New Jersey Pinelands streamflow through hydrograph analysis. Hydrological Processes 21, 185–197.
Dracup, J., 2005. Climate Change and Water Supply Reliability. Public Interest Energy Research Program (PIER), Publication Number CEC-500-2005-053, California Energy Commission, California Climate Change Center Series # 2005-014, p. 3. <http://www.energy.ca.gov/pier/project_reports/CEC-500-2005-053.html>.
Enfield, D.B., Mestas-Nuñez, A.M., Trimble, P.J., 2001. The Atlantic multidecadal oscillation and its relations to rainfall and river flows in the continental US. Geophysical Research Letters 28 (10), 2077–2080.
Feddema, J.J., Oleson, K.W., Bonan, G.B., Mearns, L.O., Buja, L.E., Meehl, G.A., Washington, W.M., 2005. The importance of land-cover change in simulating future climates. Science 310, 1674–1678.
Garfin, G., Jacobs, K., Buizer, J., 2008. Beyond brainstorming: exploring climate change adaptation strategies. EOS, Transactions of the American Geophysical Union 89 (25), 227.
Gershunov, A., Cayan, D.R., 2003. Heavy daily precipitation frequency over the contiguous United States: sources of climatic variability and seasonal predictability. Journal of Climate 16, 2752–2765.
Grantz, K., Rajagopalan, B., Clark, M., Zogona, E., 2005. A technique for incorporating large-scale climate information in basin-scale ensemble streamflow forecasts. Water Resources Research 41. doi:10.1029/2004WR003467. W10410.
Gutzler, D.S., Kann, D.M., Thornbrugh, C., 2002. Modulation of ENSO-Based long-lead outlooks of Southwestern US. Winter precipitation by the Pacific decadal oscillation. Weather and Forecasting 17, 1164–1172.

Hay, L.E., 1998. Stochastic calibration of an orographic precipitation model. Hydrological Processes 12, 613–634.
Hegerl, G.C., Zwiers, F.W., Braconnot, P., Gillett, N.P., Luo, Y., Marengo Orsini, J.A., Nicholls, N., Penner, J.E., Stott, P.A., 2007. Understanding and attributing climate change. In: Solomon, S., Qin, D., Manning, M., Chen, Z., Marquis, M., Averyt, K.B., Tignor, M., Miller, H.L. (Eds.), Climate Change 2007: The Physical Science Basis. Contribution of Working Group I to the Fourth Assessment Report of the Intergovernmental Panel on Climate Change. Cambridge University Press, p. 667.
Helsel, D.R., Hirsch, R.M., 2002. Statistical Methods in Water Resources, US Geological Survey Techniques of Water Resources Investigations, Book 4, February 2009. <http://water.usgs.gov/pubs/twri/twri4a3/>.
Hereford, R., Webb, R.H., Graham, S., 2002. Precipitation history of the Colorado Plateau Region, 1900–2000. US Geological Survey Fact Sheet, 1–4.
Hidalgo, H.G., Dracup, J.A., 2003. ENSO and PDO effects on hydroclimatic variables of the Upper Colorado River Basin. Journal of Hydrometeorology 4, 5–23.
Hidalgo, H.G., 2004. Climate precursors of multidecadal drought variability in the western United States. Water Resources Research 40. doi:10.1029/2004WR003350. W12504.
IPCC, 2007. In: Solomon, S., Qin, D., Manning, M., Chen, Z., Marquis, M., Avery, K.B., Tignor, M., Miller, H.L. (Eds.), Climate Change 2007: The Physical Science Basis. Contribution of Working Group I to the Fourth Assessment Report of the Intergovernmental Panel on Climate Change. Cambridge University Press, Cambridge, United Kingdom and New York, NY, USA.
Jain, S., Hoerling, M., Eischeid, J., 2005. Decreasing reliability and increasing synchroneity of Western North American streamflow. Journal of Climate 18, 613–618.
Kerr, R.A., 2000. A North Atlantic climate pacemaker for the centuries. Science 288, 1984–1986.
Kerr, R.A., 2009. Joining forces to pump up a variable sun's climate effects. Science 325, 1058–1059.
Kim, T-W., Chulsang, Y., Ahn, A-H., 2007. Influence of climate variation on seasonal precipitation in the Colorado River Basin. Stochastic Environmental Research and Risk Assessment 22, 411–420.
McCabe, G.J., Dettinger, M.D., 1999. Decadal variations in the strength of ENSO teleconnections with precipitation in the western United States. International Journal Climate 19, 1399–1410.
McCabe, G.J., Palecki, M.A., Betancourt, J.L., 2004. Pacific and Atlantic Ocean influences on multidecadal drought frequency in the United States. Proceedings of the National Academy of Sciences 101, 4136–4141.
McCabe, G.J., Betancourt, J.L., Hidalgo, H., 2007. Associations of decadal and multidecadal sea-surface temperature variability with Upper Colorado River flow. Journal of the American Water Resources Association 43, 183–192.
Mantaua, N.J., Hare, S.R., Zhang, Y., Wallace, J.M., Francis, R.C., 1997. A Pacific interdecadal climate oscillation with impacts on salmon production. Bulletin of the American Meteorological Society 78, 1069–1079.
Marland, G.R.A., Pielke Sr., M., Apps, R., Avissar, R.A., Betts, K.J., Davis, P.C., Frumhoff, S.T., Jackson, L., Joyce, P., Kauppi, J., Katzenberger, K.G., MacDicken, R., Neilson, J.O., Niles, D.D.S., Meehl, G.A., Arblaster, J.M., 2009. A lagged warm event-like response to peaks in solar forcing in the Pacific Region. Journal of Climate 22, 3647–3660.
Meehl, G.A., Arblaster, J.M., 2009. A lagged warm event-like response to peaks in solar forcing in the Pacific Region. Journal of Climate 22, 3647–3660.
Milly, P.C.D., Betancourt, J., Falkenmark, M., Hirsch, R., Kundzewicz, Z., Lettenmaier, D., Stouffer, R., 2008. Climate change: stationarity is dead: whither water management. Science 319 (5863), 573–574.
Monaghan, K.A., Peck, M.R., Brewin, P.A., Masiero, M., Zarate, E., Turcotte, P., Ormerod, S.J., 2000. Macroinvertebrate distribution in Ecuadorian hill streams: the effects of altitude and land use. Archiv für Hydrobiologie 149, 421–440.
Neelin, J.D., Jin, F-F., Syu, H., 2000. Variations in ENSO phase locking. Journal of Climate 13, 2570–2590.
Pagano, T.P., Garen, D., Sorooshian, S., 2004. Evaluation of official Western US seasonal water supply outlooks, 1922–2002. Journal of Hydrometeorology 5, 896–909.
Pagano, T., Garen, D., 2005. A recent increase in Western US streamflow variability and persistence. Journal of Hydrometeorology 6, 173–179.
Pielke, R.A., Avissar, R., 1990. Influence of landscape structure on local and regional climate. Landscape Ecology 4, 133–155.
Quiring, S.M., Goodrich, G.G., 2008. Nature and causes of the 2002 to 2004 drought in the southwestern United States compared with the historic 1953 to 1957 drought. Climate Research 36, 41–52.
Reed, S., King, S., Koren, V., Smith, M., Zhang, Z., Wang, D., 2001. Parameterization Assistance for NWS Hydrology Models Using ArcView, Proceedings of the 21 Annual ESRI International User Conference, San Diego, CA, July 9–13, 2001.
Rosenzweig, C., Karoly, D., Vicarelli, M., Neofotis, P., Wu, Q., Casassa, G., Menzel, A., Root, T.L., Estrella, N., Seguin, B., Tryjanowski, P., Liu, C., Rawlins, S., Imeson, A., 2008. Attributing physical and biological impacts to anthropogenic climate change. Nature 453, 353–358.
Salas, J.D., Delleur, J.W., Yevjehvich, V., Lane, W.L., 1997. Applied Modeling of Hydrologic Time Series. Water Resources Publications, LLC, Littleton, CO.
Sato, T., Kondo, J., 1988. A simple model of drainage flow in a valley. Boundary-Layer Meteorology 45, 355–369.
Schoennagel, T., Veblen, T.T., Kulakowski, D., Holz, A., 2007. Multidecadal climate variability and climate interactions affect subalpine fire occurrence, Western Colorado (USA). Ecology 88, 2891–2902.
Slack, J.R., Landwehr, J.M., 1992. Hydro-Climatic Data Network: A US Geological Survey Streamflow Data Set for the United States for the Study of Climatic Variations. US Geological Survey Report 92–129, 193 pp.
Soukup, T.L., Aziz, O.A., Tootle, G.A., Piechota, T.C., Wulff, S.S., 2009. Long lead-time streamflow forecasting of the North Platte River incorporating oceanic-atmospheric climate variability. Journal of Hydrology 368, 131–142.
Stohlgren, T.J., Chase, T.N., Pielke Sr., R.A., Kittel, T.G.F., Baron, J.S., 2003. Evidence that local land use practices influence regional climate, vegetation, and stream flow patterns in adjacent natural areas. Global Change Biology 4, 495–504.
Stott, P.A., Tett, S.F.B., Jones, G.S., Allen, M.R., Mitchell, J.F.B., Jenkins, G.J., 2000. External control of 20th century temperature by natural and anthropogenic forcings. Science 290, 2133–2136.
Stull, R.B., 1988. An Introduction to Boundary Layer Meteorology. Kluwer Academic Publishers, Dordrecht, The Netherlands. pp. 1–2.
Wang, G., Schimel, D., 2003. Climate change, climate modes, and climate impacts. Annual Review of Environmental Resources 28, 1–28.
Wang, T., Ren, H., Ma, K., 2005. Climatic signals in tree ring of *Picea schrenkiana* along an altitudinal gradient in the central Tianshan Mountains, Northwestern China. Trees 19, 735–741.
Woodhouse, C.A., 2003. A 431-yr reconstruction of Western Colorado snowpack from tree rings. Journal of Climate 16, 1551–1560.